http://www.jmaterenvironsci.com /

Numerical simulation of forced convection turbulent in a channel with transverse baffles

K. Amghar*, M. A. Louhibi, N. Salhi , M. Salhi

*Laboratoire de Mécanique & Energétique LME, Faculté des Sciences, Université Mohammed Premier,
60000 Oujda, Maroc*

Abstract

This article presents the numerical modeling of dynamic and thermal behavior of turbulent forced convection in horizontal channel within a provided of baffles, represented by the obstacles for the cooling of the hot walls. The governing equations, based on the k-ε model have been used to describe the turbulence phenomena and solved by the finite volume method. The velocity and the pressure terms of momentum equations are solved by the SIMPLE algorithm. The effect of spacing between the baffles on the heat transfer enhancement was studied in detail. The results obtained show that: (i) the spacing between the baffles have direct effects on the heat transfer by forced convection, (ii) the above results suggest that a significant increase in heat transfer in a heat exchanger tube can be obtained by introducing two transverse baffle by a spacing $d_2 = 0,101$m (very little).

1. Introduction

Turbulent flow in complex geometries receives considerable attention due to its importance in many engineering applications and has been the subject of interest for many researchers. Some of these include the energy conversion systems found in some design of nuclear reactor, heat exchangers, solar collectors, cooling of industrial machines and electronic components.

Considerable work has been done, in recent years, on the investigations of the flow and heat transfer processes at the shell-side. These are of special interest in order to improve the accuracy of prediction of heat exchangers performances. Somme works are of particular interest in the improvement and the prediction of the flows around baffles .

These studies are devised as experimental and numerical techniques. An extensive experimental study of turbulent flow and heat transfer past baffles [1-3] in heat exchangers, has been performed by various authors. Among others, Patankar and Sparrow [1] solved numerically, the problem of fluid flow and heat transfer in fully developed heat exchangers, these one was equipped by isothermal plate placed transversely to the direction of flow. They found solid plates caused strong recirculation zones in the flow field. They concluded that the Nusselt number depends strongly on the Reynolds number, and it is higher in the case of fully developed then that of laminar flow regime. Demartini et al [2] conducted numerical and experimental investigations on turbulent flow inside a rectangular channel containing two rectangular baffles. They found that numerical results were in good agreement with those obtained by experiment. In conclusion, baffles play an important role in the dynamic exchangers studied. Indeed, regions of high pressure' recirculation regions 'are formed nearly to chicanes. Rajendra et al [3]. Where conducted an experimental work on study of heat transfer and friction in rectangular ducts with baffles (solid or perforated) attached to one of the broad walls. Another study was reported by Wilfried et al [4]. These authors examined experimentally turbulent flows throughout tubular heat-exchangers. The authors focused on the impact of the baffles on heat transfer, and the geometrical properties of the heat-exchanger on the overall thermal efficiency. Ahmet *et al* [5] examined the effect of the geometric parameters on the steady turbulent flow passing through a pipe with baffles. The effect of the orientation and the distance between nine baffles on the improvement of heat transfer was highlighted in this work. Another experimental investigation was carried out by Molki et al [6] to evaluate heat transfer and pressure losses in a

rectangular channel with baffles. Recently, Saim et al [7] presented a numerical study of the dynamic behavior of turbulent air flow in horizontal channel with transverse baffles. They adapted numerical finite volume method based on the SIMPLE algorithm and chose k-ε model, for treatment of turbulence. The results obtained for a case of such type, at low Reynolds number, were presented in terms of velocity and temperature fields. They found the existence of relatively strong recirculation zones near the baffles. The eddy zones are responsible of local variations in the Nusselt numbers along the baffles and walls.

NOMENCLATURE

C_1 - Turbulent constant used in the standard k-ε model
C_2- Turbulent constant used in the standard k-ε model
C_μ- Constant used in the standard k –ε model
μ_l, μ_t- laminar, turbulent viscosity, [Pa.s]
P- Pressure, [Pa]
T- Temperature, (K)
δ -Width of baffles, [m]
U_0-Inlet velocity [m/s]
u, v - Fluid velocity in the x- and y-direction,[m/s]
T_{int} - Inlet temperature (°C)

Re -Reynolds number (= $\rho D_h U_0/\mu$)
k - turbulent kinetic energy, [m²/s²]
υ- kinematics viscosity, [m²/s]
μ_e- effective viscosity, [Pa·s]
L -channel length, [m]
u_{int} - inlet velocity [m/s]
$d_{i=1,3}$- distance between two baffles, [m]
$S_\emptyset$- limit of source for the general variable
L_1-distance upstream of the first baffle,[m]
h- baffle height, [m]

Greek symbols

N_μ- Local Nusselt number
G - Flow production term.
D_h- Hydraulic diameter, [m]
H - Channel height, [m]
f_μ - Modeling damping functions for the LRN k-ε model
$Γ_\Phi$- diffusion coefficient

ρ- density of the air [Kg/m^3]
in, out - inlet, outlet of the test section
Φ - Stands for the dependent used u,v,T, k and ε
σ_K,σ_ε ,σ_T- turbulence model constant for k, ε
and T

Subscripts and Superscripts

ε- dissipation rate of turbulence energy,[m²/s²]
f - fluid
t – turbulent
w - wall
e – effective
SIMPLE- Semi-implicit method for pressure-linked equations

The main objective of the present work is to investigate the forced turbulent convection in a two-dimensional channel containing two baffles placed on the lower wall. To carry out this study, we have used a thermal model. The analysis of the turbulent flow of the air in this channel allows to understand the dynamic and thermal comportment from a channel, to knowing upstream ,downstream and between the two baffles. For the different placement between the baffles are presented and a special interest is given to the influence of the Nusselt number. The simulation results are then analyzed to explain this real application in the field of heat exchangers and their importance in the industry. The remainder of this article presents, in section 2, a presentation of the physical model and a brief description of the mathematical formulation. Section 3 is dedicated to the numerical technique. Section 4 is devoted to the presentation and comments of the obtained results. Then, a general conclusion will be presented.

2. Mathematical modeling and analysis

2.1. *Description of the physical model*

The geometry of the problem is presented on (**Fig 1**). Is a rectangular duct with isothermal horizontal walls, crossed by a stationary turbulent flow. The physical properties are considered to be constants. In this numerical investigation, the following hypotheses are adopted:

(i) Physical properties of air are constant.
(ii) A profile of velocity is uniform at the inlet.
(iii) The radiation heat transfer is negligible.
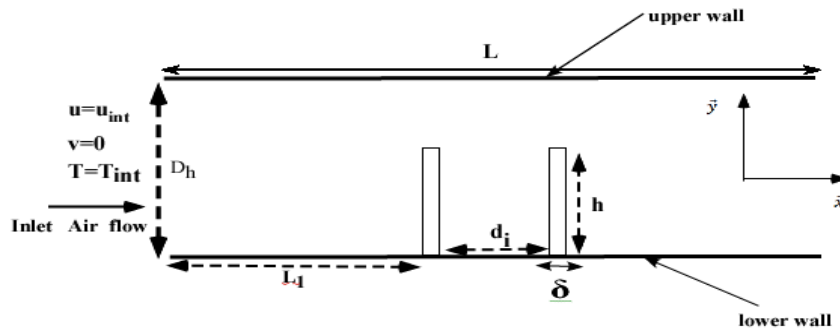(iv)The flow is assumed to be steady.

Fig 1: The geometry of the system under investigation: Plate baffles

2.2. Mathematical modeling

Under these conditions, transport equations that describe the principle of conservation of matter and momentum can be written in the following form Patankar [8]:

$$\frac{\partial(\rho u\Phi)}{\partial x} + \frac{\partial(\rho v\Phi)}{\partial y} = \frac{\partial}{\partial x}\left[\Gamma_\phi \frac{\partial \Phi}{\partial x}\right] + \frac{\partial}{\partial y}\left[\Gamma_\phi \frac{\partial \Phi}{\partial y}\right] + S_\phi \tag{1}$$

Φ is a vector composed of the scalars u, v, k and ε.

u and v stand for the mean velocities towards the axis x and y respectively.

k and ε stand for kinetic energy and turbulent dissipation respectively.

Γ_ϕ and S_ϕ represent the coefficient of turbulent diffusion and the source term associated with the variable ϕ, The expressions of Φ, Γ_ϕ and S_ϕ are presented for.

- The continuity equation :

$\phi = 1$

$\tau_\phi = 0$

$S_\phi = 0$

The continuity equation is given by:

$$\frac{\partial}{\partial x}(\rho u) + \frac{\partial}{\partial y}(\rho v) = 0 \tag{2}$$

- The momentum equation in X-direction :

$\phi = u$

$\tau_\phi = \mu_e$

$S_\phi = -\frac{\partial P}{\partial x}$

The momentum equation in X-direction is given by:

$$\frac{\partial}{\partial x}(\rho u^2) + \frac{\partial}{\partial y}(\rho uv) = -\frac{\partial P}{\partial x} + \frac{\partial}{\partial x}\left[(\mu_l + \mu_t)(\frac{\partial u}{\partial x})\right] + \frac{\partial}{\partial y}\left[(\mu_l + \mu_t)\left(\frac{\partial u}{\partial y}\right)\right] \tag{3}$$

- The momentum equation inY-direction :

$\phi = v$

$\tau_\phi = \mu_e$

$S_\phi = -\frac{\partial P}{\partial y}$

The momentum equation in Y-direction is given by:

$$\frac{\partial}{\partial x}(\rho uv) + \frac{\partial}{\partial y}(\rho v^2) = -\frac{\partial P}{\partial y} + \frac{\partial}{\partial x}\left[(\mu_l + \mu_t)\left(\frac{\partial v}{\partial x}\right)\right] + \frac{\partial}{\partial y}\left[(\mu_l + \mu_t)\left(\frac{\partial v}{\partial y}\right)\right] \tag{4}$$

- The energy equation :

$$\phi = T$$

$$\tau_\phi = \mu_l + \frac{\mu_t}{\sigma_T}$$

$$S_\phi = 0$$

The energy equation is given by:

$$\frac{\partial}{\partial x}\left(\rho u T\right) + \frac{\partial}{\partial y}\left(\rho v T\right) = \frac{\partial}{\partial x}\left[\left(\mu_l + \frac{\mu_t}{\sigma_T}\right)\frac{\partial T}{\partial x}\right] + \frac{\partial}{\partial y}\left[\left(\mu_l + \frac{\mu_t}{\sigma_T}\right)\left(\frac{\partial T}{\partial y}\right)\right] \qquad (5)$$

- Turbulent energy equation :

$$\phi = k$$

$$\tau_\phi = \mu_l + \frac{\mu_t}{\sigma_k}$$

$$S_\phi = -\rho\varepsilon + G$$

The turbulent energy equation is given by:

$$\frac{\partial}{\partial x}\left(\rho u K\right) + \frac{\partial}{\partial y}\left(\rho v K\right) = \frac{\partial}{\partial x}\left[\left(\mu_l + \frac{\mu_t}{\sigma_K}\right)\left(\frac{\partial K}{\partial x}\right)\right] + \frac{\partial}{\partial y}\left[\left(\mu_l + \frac{\mu_t}{\sigma_K}\right)\left(\frac{\partial K}{\partial y}\right)\right] - \rho\varepsilon + G \qquad (6)$$

- The turbulent dissipation equation :

$$\phi = \varepsilon$$

$$T_\phi = \mu_l + \frac{\mu_t}{\sigma_\varepsilon}$$

$$S_\phi = 0$$

The turbulent dissipation equation is given by:

$$\frac{\partial}{\partial x}(\rho u \varepsilon) + \frac{\partial}{\partial y}(\rho v \varepsilon) = \frac{\partial}{\partial x}\left[\left(\mu_l + \frac{\mu_t}{\sigma_\varepsilon}\right)\left(\frac{\partial \varepsilon}{\partial x}\right)\right] + \frac{\partial}{\partial y}\left[\left(\mu_l + \frac{\mu_t}{\sigma_\varepsilon}\right)\left(\frac{\partial \varepsilon}{\partial y}\right)\right] \qquad (7)$$

Where, for a 2-D, the flow production term becomes:

$$G = \mu_t\left[2\left(\frac{\partial u}{\partial x}\right)^2 + 2\left(\frac{\partial v}{\partial y}\right)^2 + \left(\frac{\partial v}{\partial x} + \frac{\partial u}{\partial y}\right)^2\right]$$

μ_l and μ_t represent, respectively, the laminar and turbulent viscosities.

$$\mu_e = \mu_l + \mu_t$$

$$\mu_t = f_\mu . \rho . c_\mu . \frac{K^2}{\varepsilon}$$

The turbulent constants correspond to those suggested by Launder and spalding [9] and Chieng et al [10] These constants are arranged in the table below (**Table** 1).

Table 1: Turbulent constant in the governing equations

C_μ	C_1	C_2	σ_T	σ_k	σ_ε
0,09	1,44	1,92	0,9	1	1,3

2.3 .Boundary conditions:

A fully developed turbulent flow is considered. The quantities K, ε are obtained by using numerical calculations based on the k-ε, model.

The boundary conditions are listed below:

1- At the inlet of the channel:

$$u = u_{int} = 7,8m/s \ , \ v = 0$$

$$K_{in} = 0,005U^2_{in}$$

$$\varepsilon_{in} = 0,1K^2_{in}$$

$$T_{in} = 300K$$

K_{in} Stands for the admission condition for turbulent kinetic energy, and ε_{in} is the inlet condition for dissipation.

2- At the walls:

$$u = v = 0, K = \varepsilon = 0$$

$$T = T_W = 373K$$

3- At the exit: all gradients are null.

$$\frac{\partial u}{\partial x} = \frac{\partial v}{\partial x} = \frac{\partial K}{\partial x} = \frac{\partial \varepsilon}{\partial x} = \frac{\partial T}{\partial x} = 0$$

$$P = P_{atm}$$

2.4. Mathematical Resolution

The discretization consists to transform a transport differential equation into a system of algebraic equations. As shown by the following mesh, the integration of the equation (1) is done on the control volume (square mesh) of center P, (**Fig 2**).
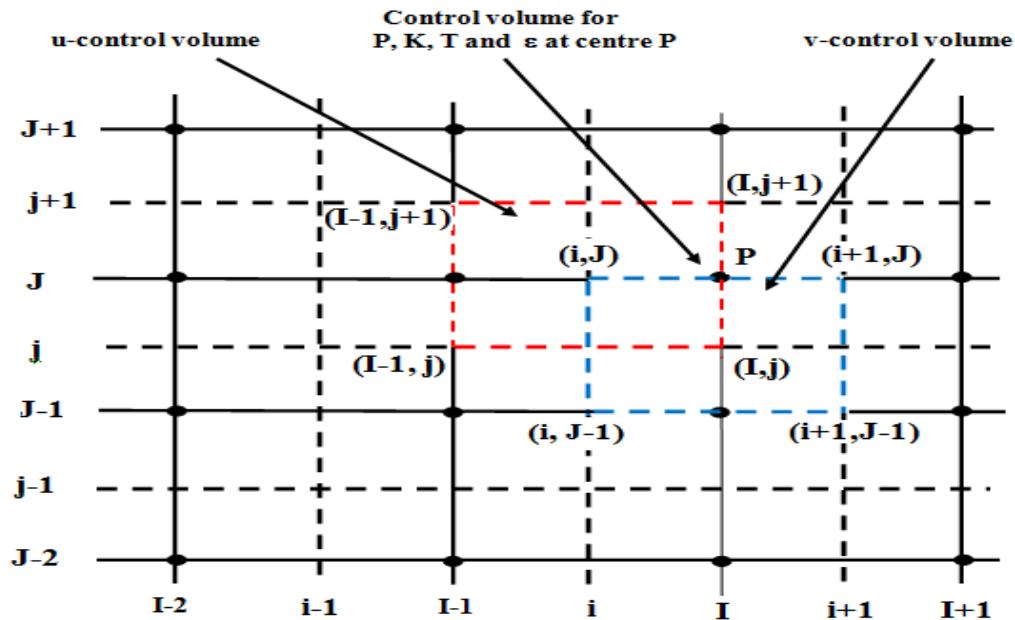

Fig 2: Two-dimensional control volume (Square mesh)

Then, the transport equation (1) can be written from:

$$\rho u\phi_e - \rho u\phi_w + \rho v\phi_n - \rho v\phi_s = \tau_\phi(\frac{\partial \phi}{\partial x})_e - \tau_\phi(\frac{\partial \phi}{\partial x})_w + \tau_\phi(\frac{\partial \phi}{\partial y})_n - \tau_\phi(\frac{\partial \phi}{\partial y})_s + \int_v S_\phi dv \qquad (8)$$

$$D_e = \frac{\tau_\phi}{\Delta x} \qquad , \qquad D_w = \frac{\tau_\phi}{\Delta x} \qquad , \qquad (\frac{\partial \phi}{\partial x})_e = \frac{\phi_E - \phi_P}{\Delta x}$$

$$D_s = \frac{\tau_\phi}{\Delta y} \quad , \quad D_n = \frac{\tau_\phi}{\Delta y} \quad , \quad (\frac{\partial \phi}{\partial x})_w = \frac{\phi_P - \phi_w}{\Delta x}.$$

$$F_e = \rho u_e \quad , \quad F_n = \rho v_n \quad , \quad (\frac{\partial \phi}{\partial y})_y = \frac{\phi_N - \phi_P}{\Delta y}$$

$$F_w = \rho u_w \quad , \quad F_s = \rho v_s \quad , \quad (\frac{\partial \phi}{\partial y})_s = \frac{\phi_P - \phi_S}{\Delta y}$$

Hence, the expression of equation (8) becomes:

$$F_e \phi_e - F_w \phi_w + F_n \phi_n - F_s \phi_s = D_e(\phi_E - \phi_P) - D_w(\phi_P - \phi_w) + D_n(\phi_N - \phi_P) - D_s(\phi_P - \phi_s) + \int_V S_v Dv \qquad (9)$$

The value of φ on the faces e, w, n and s can be given by scheme "Quick" (Quadratic upwind differencing scheme), which proposes to approximate the variation of the variable Φ, by a quadratic interpolation where uses a three point upstream weighted quadratic interpolation for cell face values: 2 bracketing nodes and one in the further upstream side.
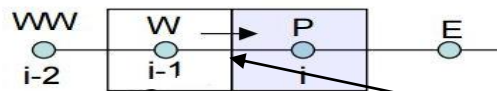
$$\phi_{face} = \frac{6}{8}\phi_{i-1} + \frac{3}{8}\phi_i - \frac{1}{8}\phi_{i-2}$$

When, $u_w > 0$ and $u_e > 0$ a quadratic fit through WW, W and P is used to evaluate $\emptyset_w$, and a further quadratic fit through W, P and E to calculate $\emptyset_e$ (**Fig 2**).
And when, $v_s > 0$ and $v_n > 0$ values of φ at S, P and SS are used for $\emptyset_s$, and values at P, N and S for $\emptyset_n$ (**Fig 2**).
It can be shown that for a uniform grid the value of at the cell face between two bracketing nodes i and $i-1$ and upstream node $i-2$ is given by the following formula:

$$\phi_{face} = \frac{6}{8}\phi_{i-1} + \frac{3}{8}\phi_i - \frac{1}{8}\phi_{i-2}$$

When, $u_w > 0$, the bracketing nodes for the west face w are W and P, the upstream node is WW.

$$\phi_w = \frac{6}{8}\phi_W + \frac{3}{8}\phi_P - \frac{1}{8}\phi_{WW} \qquad (10)$$

When, $u_e > 0$, the bracketing nodes for the east face e are P and E, the upstream node is W, so:

$$\phi_e = \frac{6}{8}\phi_P + \frac{3}{8}\phi_E - \frac{1}{8}\phi_W \qquad (11)$$

The same thing is done for the vertical "y" direction, using the faces "n" and "s" and by introducing the Quick diagram nodes N, NN, S and SS (**Fig 2**).

$$\phi_n = \frac{6}{8}\phi_P + \frac{3}{8}\phi_N - \frac{1}{8}\phi_S \qquad (12) \qquad , \qquad \phi_s = \frac{6}{8}\phi_S + \frac{3}{8}\phi_P - \frac{1}{8}\phi_{SS} \qquad (13)$$

Finally, the equation (9) is discretized on the mesh with P at center, where as the direction of flow on these faces as ($u_e > 0, u_w > 0, v_n > 0, v_s > 0$).

$$a_p \phi_p = a_E \phi_E + a_w \phi_w + a_N \phi_N + a_s \phi_s + a_{WW} \phi_{WW} + a_{SS} \phi_{SS} + \int_v S_{\phi x} dv \qquad (14)$$

With:
$$\begin{cases} a_E = D_e - \frac{3}{8}F_e \\ a_w = D_w + \frac{1}{8}F_e + \frac{6}{8}F_w \\ a_{N=D_n-\frac{3}{8}F_n} \\ a_S = D_s + \frac{1}{8}F_n + \frac{6}{8}F_s \end{cases}$$
and neighbour coefficients,
$$\begin{cases} a_{ww} = -\frac{1}{8}F_w \\ a_{SS} = -\frac{1}{8}F_s \\ a_p = a_E + a_W + a_N + a_S + a_{WW} + a_{SS} \\ \qquad + (F_e - F_w) + (F_n - F_s) \end{cases}$$

For, $u_w < 0$, $u_e < 0$, $v_n < 0$ and $v_s < 0$, the flux across the west, east, north and south boundaries is given by the expressions, (**Fig 2**):

$$\phi_e = \frac{6}{8}\phi_E + \frac{3}{8}\phi_P - \frac{1}{8}\phi_{EE} \qquad (15) \qquad\qquad , \qquad\qquad \phi_w = \frac{6}{8}\phi_P + \frac{3}{8}\phi_W - \frac{1}{8}\phi_E \qquad (16)$$

$$\phi_n = \frac{6}{8}\phi_N + \frac{3}{8}\phi_P - \frac{1}{8}\phi_{NN} \qquad (17) \qquad\qquad , \qquad\qquad \phi_s = \frac{6}{8}\phi_P + \frac{3}{8}\phi_S - \frac{1}{8}\phi_N \qquad (18)$$

Substitution of these formulae (15, 16, 17, 18), for the convective terms in the discretised equation (9), after rearrangement, we obtain the following formula.

$$a_P\phi_P = a_E\phi_E + a_W\phi_W + a_{EE}\phi_{EE} + a_{NN}\phi_{NN} + a_S\phi_S + a_N\phi_N + \int_v S_{\phi y}\,dv \qquad (19)$$

With: $\begin{cases} a_w = D_w - \frac{3}{8}F_w \\ a_E = D_e + \frac{1}{8}F_w + \frac{6}{8}F_e \\ a_N = D_n + \frac{1}{8}F_s + \frac{6}{8}F_n \\ a_S = D_s - \frac{3}{8}F_s \end{cases}$ and, $\begin{cases} a_{EE} = -\frac{1}{8}F_e \\ a_{NN} = -\frac{1}{8}F_n \\ a_P = a_W + a_E + a_N + a_{EE} + a_S + a_{NN} \\ \qquad + (F_w - F_e) + (F_s - F_n) \end{cases}$

General expressions, valid for positive and negative flow directions, can be obtained by combining the two sets of coefficients above. The QUICK scheme for the transport equation problems (1) can be summarized as follows:

$$a_P\phi_P = a_E\phi_E + a_W\phi_W + a_N\phi_N + a_S\phi_S + a_{EE}\phi_{EE} + a_{WW}\phi_{EE} + a_{NN}\phi_{NN} + a_{SS}\phi_{SS} + \int_v S_\phi\,dv \qquad (20)$$

With central coefficient:

$$a_P = a_E + a_W + a_N + a_S + a_{EE} + a_{WW} + a_{NN} + a_{SS} \qquad (21)$$

and neighbour coefficients : $\begin{cases} a_E = D_e - \frac{3}{8}\alpha_e F_e + \frac{1}{8}(1-\alpha_w)F_w + \frac{6}{8}(1-\alpha_e)F_e \\ a_w = D_w + \frac{1}{8}\alpha_e F_e + \frac{6}{8}\alpha_w F_w - \frac{3}{8}(1-\alpha_w)F_w \\ a_N = D_n - \frac{3}{8}\alpha_N F_N + \frac{1}{8}(1-\alpha_s)F_s + \frac{6}{8}(1-\alpha_n)F_n \\ a_S = D_s + \frac{1}{8}\alpha_n F_n + \frac{6}{8}\alpha_s F_s - \frac{3}{8}(1-\alpha_s)F_s \\ a_{EE} = -\frac{1}{8}(1-\alpha_e)F_e \\ a_{WW} = -\frac{1}{8}\alpha_w F_w \\ a_{NN} = -\frac{1}{8}(1-\alpha_n)F_n \\ a_{SS} = -\frac{1}{8}\alpha_s F_s \end{cases}$

Where:

$\alpha_w = 1$ for $u_w > 0$ and $\alpha_e = 1$ for $u_e > 0$
$\alpha_w = 0$ for $u_w < 0$ and $\alpha_e = 0$ for $u_e < 0$
$\alpha_n = 1$ for $u_n > 0$ and $\alpha_s = 1$ for $u_s > 0$
$\alpha_n = 0$ for $u_n < 0$ and $\alpha_s = 0$ for $u_s < 0$

Finally, the discritization of the flow domain by the finite volume method on the control volume [(I, j); $(I, j -1)$; $(I -1, j -1)$; $(I -1, j)$], (**Fig 2**), where, $\phi = u$. the algebraic equation can be written as:

$$a_{i,J}u_{i,J} = \sum_{nb} a_{nb}u_{nb} + [P(I-1,J) - P(I,J)](y_{j+1} - y_j) \qquad (22)$$

Where:

$$\sum_{nb} a_{nb}u_{nb} = a_{i-2,J}u_{i-2,J} + a_{i-1,J}u_{i-1,J} + a_{i+1,J}u_{i+1,J} + a_{i+2,J}u_{i+2,J} + a_{i,J+1}u_{i,J+1} + a_{i,J+2}u_{J+2}$$

$$+ a_{i,J-1}u_{J-1} + a_{i,J-2}u_{J-2} \qquad (23)$$

Similarly, the integration of the conservation of momentum equation in the vertical direction « v » in the volume $[(i+1, J-1); (i+1, J); (i, J); (i-1, J-1)]$, (**Fig 2**) give as:

$$a_{I,j}v_{I,j} = \sum_{nb} a_{nb}v_{nb} + [P(I, J-1) - P(I, J)](x_{i+1} - x_i) \qquad (24)$$

Where:

$$\sum_{nb} a_{nb}v_{nb} = a_{I+1,j}v_{I+1,j} + a_{I+2,j}v_{I+2,j} + a_{I-1,j}v_{I-1,j} + a_{I-2,j}v_{I-2,j} + a_{I,j-1}v_{I,j-1} + a_{I,j-2}v_{I,j-2}$$

$$+ a_{I,j+1}v_{I,j+1} + a_{I,j+2}v_{I,j+2} \qquad (25)$$

Therefore, the general algebraic equation can be written as:

$$a_{i,j}\phi_{i,j} = a_{i+1,j}\phi_{i+1,j} + a_{i+2,j}\phi_{i+2,j} + a_{i-1,j}\phi_{i-1,j} + a_{i-2,j}\phi_{i-2,j} + a_{i,j+1}\phi_{i,j+1} + a_{i,j+2}\phi_{i,j+2}$$

$$+ a_{i,j-1}\phi_{i,j-1} + a_{i,j-2}\phi_{i,j-2} + b_{i,j} \qquad (26)$$

3. Numerical Resolution

The governing equations describe the flow and heat transfer in this problem, are solved by the finite volume method (FVM), based on the algorithm SIMPLE (Semi-implicit method for pressure-linked equations) [11], for the coupling pressure-velocity, taking into account the characteristics the air flow, the numerical the schema Quick [12], was applied to the interpolations and since the system is a second order it was used for the terms of pressure. Therefore, the general algebraic equation can be written as:

$$a_{i,j}\phi_{i,j} = a_{i+1,j}\phi_{i+1,j} + a_{i+2,j}\phi_{i+2,j} + a_{i-1,j}\phi_{i-1,j} + a_{i-2,j}\phi_{i-2,j} + a_{i,j+1}\phi_{i,j+1} + a_{i,j+2}\phi_{i,j+2}$$

$$+ a_{i,j-1}\phi_{i,j-1} + a_{i,j-2}\phi_{i,j-2} + b_{i,j} \qquad (26)$$

A structured grid element with the quadrilateral type is used because it is considered to be more adequate for the suggested geometry. The Numerical simulations are tested by varying the number of elements of mesh and the results show that the stability of convergence of the model is achieved for all meshes.

The iterative solution is continued until the residuals for all cells of calculation have become less than 10^{-5} for all dependent variables.

4. Results and discussion

For the numerical simulations presented in this work, we refer to the experimental work done by (Demartini et al. 2004), who studied the baffles transversal .

The geometric dimensions of the system are listed below:

- length of the channel $L = 0.554$ m,
- height of the channel $H = 0.146$ m,
- thickness of the baffle $\delta = 0.08$ m,
- height of the baffle h= 0.1 m,
- distance between the intake of the channel and the first baffle $L_1 = 0.218$ m,
- reynolds number $Re = 8.73\ 10^4$
- hydraulic diameter of the channel $D_h = 0.167$ m, and
- Velocity of air particles at the inlet $U_0 = 7.8$ m/s.

Numerically, we used a constant mesh of (200 x 90) in the vertical and horizontal directions respectively. They proved to be sufficient to the model of the system. The meshing size is comparatively smaller near to the boundaries of the baffles, so a good estimate of the gradients can be obtained.

We first studied the flow along the channel containing two baffles placed a lower wall to put in evidence the influence of the spacing of the baffles on heat exchange.

Both baffles have the same height (h = 0.1 m), the first baffle is placed at $L_1 = 0.15\ m$ distance, while the second is placed at $d_1 = 0.05$m distance from the first (case 1), $d_2 = 0.10$ m (case 2) and $d_3 = 0.15$ m (case3).

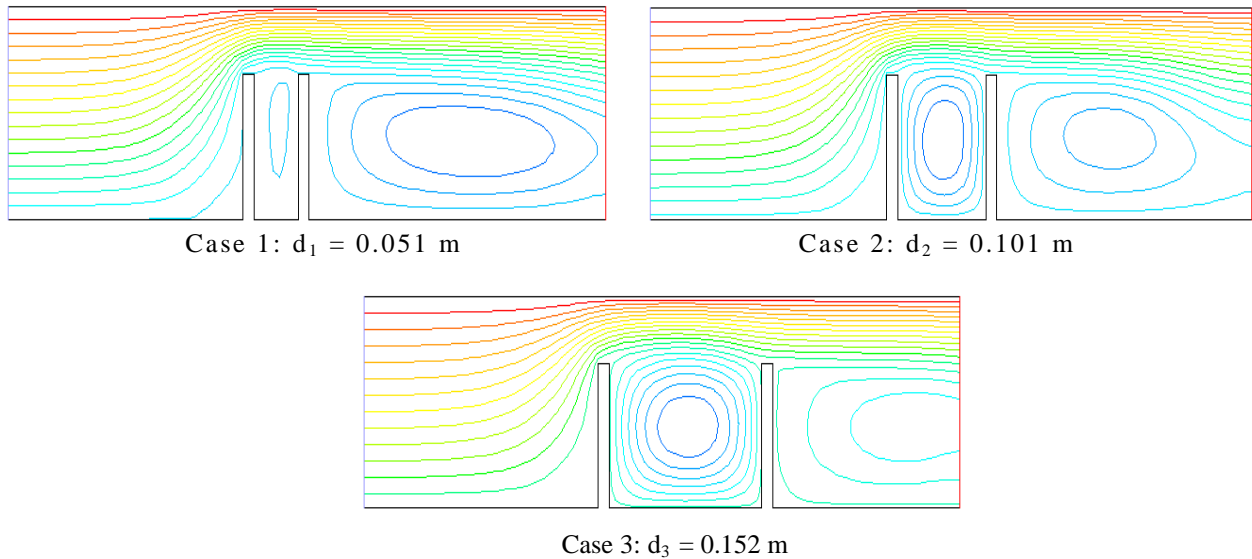The streamlines for the three cases are presented in (**Fig 3**):

Case 1: $d_1 = 0.051$ m Case 2: $d_2 = 0.101$ m

Case 3: $d_3 = 0.152$ m

Fig 3: Streamlines for the different spacing for both baffles

We first find the existence of two recirculation zones in a downstream of the second baffle and the other between both of them. The analysis of the results show the increase of the recirculation zone between the two baffles when the variation of spacing is increasing. While second recirculation zone in a downstream of the second baffle decreases with the decrease of the distance between the second baffles and the outlet of the channel.

In fact , when the two baffle are close to each other ' d_1 small',the fluid is blocked between the two baffles therefore the velocity is decreasing in this spacing. Consequently, there will be a decrease in the heat transfer in this zone but an increase of d_1.Hence ,the fluid has sufficient space to circulate quickly then increases the heat transfer in this zone **'Fig 4'**.
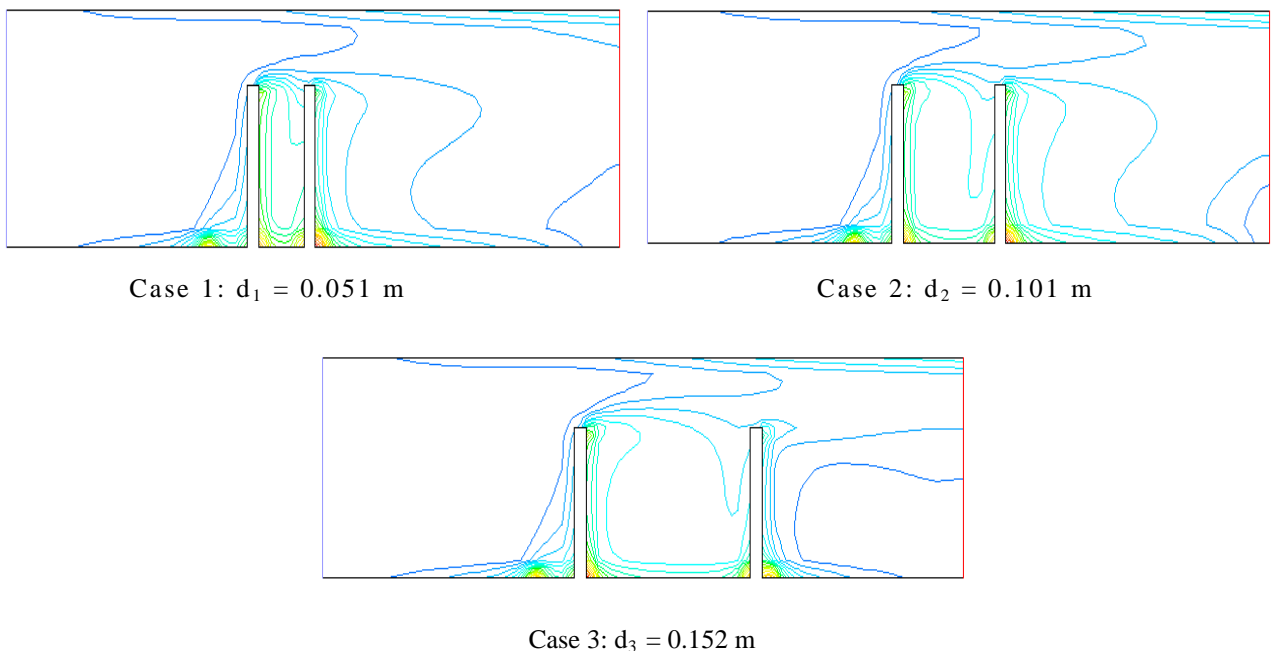

Case 1: $d_1 = 0.051$ m Case 2: $d_2 = 0.101$ m

Case 3: $d_3 = 0.152$ m

Fig 4: Isotherms for different spacing for the two baffles

Figures 5 and **6** show the Profiles of the horizontal velocity and the temperature distribution respectively for the three different spacing d_1, d_2, d_3, between the two baffles, along the diameter of channel at the inlet in the downstream located at position x = 0,45m.

This figure shows the distribution of the axial velocity at the position x = 0,45m.We observed a decrease of the velocity until it reaches its negative values in the lower region of the channel. The values decrease with decreasing spacing between the two baffles (but very little).

Also in the lower part of the channel, the negative velocity indicates the presence of recirculation zone of the flow formed behind the second obstacles. This field decreases with decreasing the distance between the second baffle and the channel outlet.
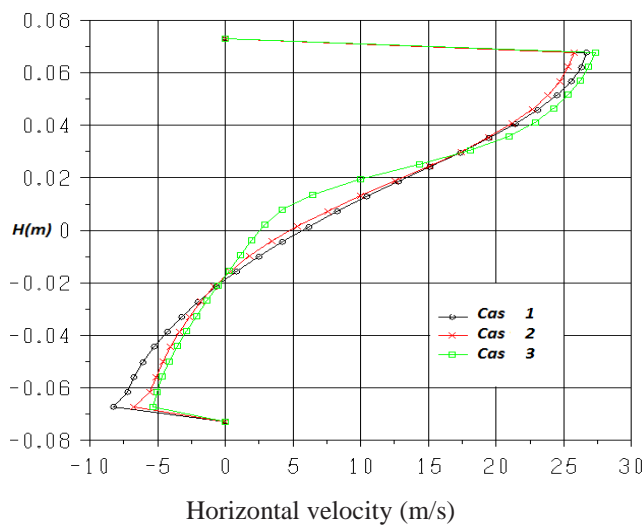

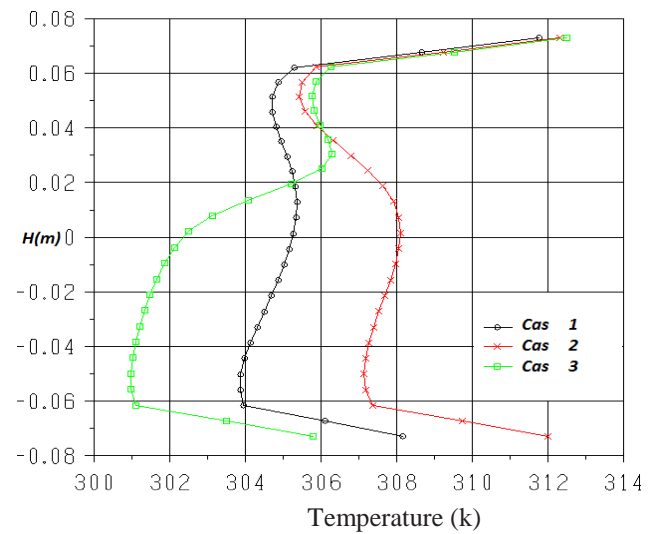**Fig 5:** Profiles of horizontal velocity u downstream of the second baffle at x=0,45 m

Fig 6: Profiles of temperature of the second baffle at x=0,45 m

In the upper half of the channel, the flow is characterized by very high velocity which can reach 340% in the inlet velocity. The results show that the maximum values of the flow velocity are observed in the case where the spacing between the two baffles is the largest (but very little).

We notice that the flow is characterized by the temperatures of high air for the case with average spacing between the two baffles, which means $d_2 = 0.101$ m, compared with the case of the small spacing $d_1 = 0.051$ m (Fig.6).

For the case of the spacing $d_3 = 0.152$ m, we observed a more important decrease of the temperature, in comparison to the two other cases spacing in the lower part of the channel. These effects become negligible in the upper part of the channel. The numerical results show the relevance of the intermediate case where the spacing is $d_2 = 0.101$ m.

This remark is still apparent if we observe the local Nusselt number along the wall (**Fig 7**), where we represent the local Nusselt number along the channel for the three spacing considered« $d_1 = 0.051$ m ; $d_2 = 0.101$ m and $d_3 = 0.152$ m ».
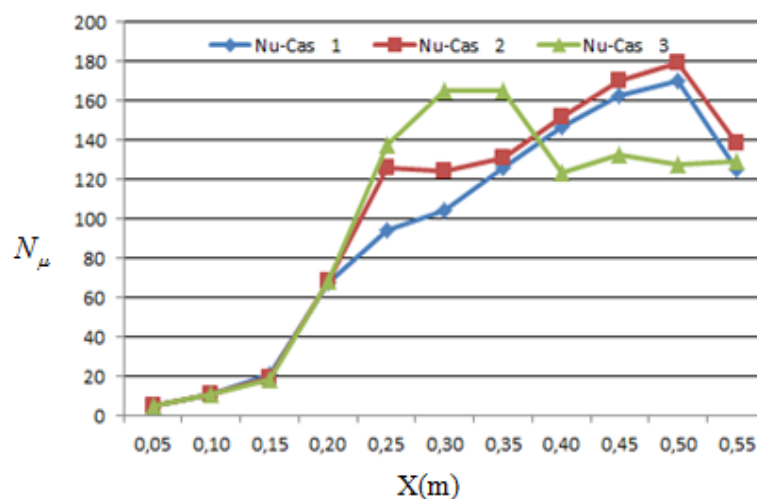

Fig 7: Local Nusselt number along the channel «Effect of the spacing between the two baffles»

The same transfer rate was observed before reaching the abscise corresponding abscise at the top of the first baffle. The heat transfer is more important between the two baffles if the spacing is greater. Beyond the second baffle, we acknowledge a more important transfer of the second case $d_2 = 0.101$ m.

Conclusion

The contribution to the study of a turbulent flow in forced convection inside a channel equipping the baffles in the lower wall is carried out. The numerical results obtained by the finite volume method, are presented to analyze the results of a turbulent flow using the model k-ε. The results obtained by our code show the dynamic and thermal behavior for different geometric situation.

The main objective of our work is to study the effect of spacing between the baffles on the heat exchange between hot solid wall and the flow. It can be concluded that the spacing between the baffles plays an important role in improving the heat transfer. The spacing of d_1 between the baffles has different effects on local heat transfer within the concerned zone.

However ; the spacing of d_1 doesn't have much influence on the overall heat transfer within the channel, so we observed the relevance of the intermediate case where the spacing $d_2 = 0.101$m.Finally,we plan to exploit our results and then try to apply this code to other geometrically complicated situations (Non-rectangular baffles or inclined baffles).

References

1. PatankaS.V. Sparrow E.M., *Journal of Heat Transfer,* 99 (1977) 180 -6),
2. Demartini L.C., Vielmo H.A., Moller S.V., J. *Braz. Soc. Mech. Sci. & Eng,* XXVI, No. 2 (2004) 153-159
3. Rajendra K., Maheshwarib B.K. and Nitin K., 'Experimental Study of Heat Transfer Enhancement in an Asymmetrically Heated Rectangular Duct with Perforated Baffles', *International Communications in Heat and Mass Transfer,* 32, N°1-2 (2005) 275 - 284.
4. Wilfried R. and Deiying W. L., Effect of baffle/shell leakage flow on heat transfer in shell-and-tube heat exchanger, *Experimental Thermal and Fluid Science*, 8 (1994) 10-20.
5. Ahmet Tandiroglu, Effect of flow geometry parameters on transient heat transfer for turbulent flow in a circular tube with baffle inserts, *International Journal of Heat and Mass Transfer,* 49 (2006) 1559–1567
6. Molki M. and Mostoufizadeh A.R., 'Turbulent Heat Transfer in Rectangular Ducts with Repeated-Baffle Blockage*s*', *international Journal of Heat and Mass Transfer,* 32, N°8 (1989) 1491 - 1499,
7. Saim R., Abboudi S., Benyoucef B., Azzi A., algériens Journal de mécanique des fluides appliquée / vol 2/2007 (ISSN 1718 - 5130).
8. Patankar S.V., Numerical Heat Transfer and Fluid Flow, Hemisphere, New York, USA, 1980
9. Launder B.E., Spalding D.B., The numerical computation of turbulent flow, *Computer Methods in Applied Mechanics and Engineering,* 3 (1974) 269-289.
10. Chieng C.C et Launder B.E., *Numérique de transfert de chaleur,* vol. 3, pp. 189-207.
11. Van Doormal J. P., Raithyb G.D., "Enhancements of the SIMPLE Method for Predicting Incompressible Fluid Flow", *Numerical Heat Transfer,* 7 (1984) 147-163.
12. Versteeg H.K., and Malalasekera W., (1995), an introduction to Computational Fluid Dynamics, The finite volume method, Addison Wesley Longman Limited, England.

(2017) ; http://www.jmaterenvironsci.com